Journal of Sound and Vibration 330 (2011) 947–954

Contents lists available at ScienceDirect

Journal of Sound and Vibration

journal homepage: www.elsevier.com/locate/jsvi

A nonlinear constitutive audio frequency magneto-sensitive rubber model including amplitude, frequency and magnetic field dependence

Peter Blom, Leif Kari *

The Marcus Wallenberg Laboratory for Sound and Vibration Research, Royal Institute of Technology, 10044 Stockholm, Sweden

ARTICLE INFO

Article history:
Received 6 June 2007
Received in revised form
6 June 2010
Accepted 13 September 2010
Handling Editor: M.P. Cartmell
Available online 15 October 2010

ABSTRACT

A novel constitutive model of magneto-sensitive rubber in the audible frequency range is presented. Characteristics inherent to magneto-sensitive rubber within this dynamic regime are defined: magnetic sensitivity, amplitude dependence, elasticity and viscoelasticity. Prior to creating the model assumptions based on experimental observations concerning these components are formulated. The first observation is that not only does the rubber display a strong amplitude dependence even for small strains, but also the magnetic sensitivity is strongly amplitude dependent. The second and third are, respectively, that the elastic component is magneto-sensitive, whereas the viscoelastic dependence on magnetic induction appears to be small. Thus, the model is developed from these assumptions and parameters are optimized with respect to experimental values for one case and subsequently validated for others; a very good agreement is obtained.

1. Introduction

The term intelligent or smart materials was coined some 20 years ago and has become a common denominator in fields previously considered disparate—such as medicine and mechanics—by linking mechanical, physical and chemical properties. It is through the possibility to alter one material property to obtain a change in another one, thus seaming together functions of materials that have previously served separate purposes, that new dimensions arise in terms of material behaviour. Narrowing the wide concept of intelligent materials down to one certain subclass, namely that of magneto-sensitive materials (MS), research was started in the end of the 40s by Rabinow [1] who was working on magneto-sensitive fluids while concurrently Winslow [2] was working on electro-sensitive (ES) fluids. In response to their discoveries research on MS and ES materials gained momentum, but focus has until recently remained on ES materials. Nevertheless, MS materials have proven more commercially successful and over the last years their large potential have been widely recognized; this has lately prompted a large number of research reports on MS fluids and solids alike [3–11]. Magneto-sensitive rubber has become the subject of much research because of the wide presence of rubber in applications such as for instance bushings and engine mounts; the interest lies in the capability to dynamically change the rubber sample stiffness and damping, achieved by applying a magnetic field over a rubber sample containing iron particles. The application of a magnetic field gives rise to a magnetic dipole–dipole interaction between the iron particles causing the apparent changes in stiffness and damping.

The quasi-static behaviour of MS rubber has lately been studied extensively [12–17]. On the other hand, the dynamic properties, ranging into the audible frequency range, have been given less attention. No models known to the authors include

* Corresponding author. Tel.: +46 8 7907974; fax: +46 8 7906122.
E-mail addresses: pblom@kth.se (P. Blom), leifkari@kth.se (L. Kari).

0022-460X/$ - see front matter © 2010 Elsevier Ltd. All rights reserved.
doi:10.1016/j.jsv.2010.09.010

viscoelasticity in their theories. Nonetheless, considering the above mentioned examples of engine mounts and bushings—these are frequently subjected to vibrations ranging far into the audio frequency range—merely the quasi-static properties are not sufficient in describing the rubber behaviour. Because of the viscous nature of rubber the viscoelastic characteristics need also be incorporated in order to properly describe its complex characteristics. Another rubber feature that arises from a phenomenon referred to as the Fletcher–Gent effect [18]—the dependence of stiffness on strain amplitude—has so far been omitted from MS models in general. Neglecting its influence is normally justified for unfilled rubber subject only to small strains. However, in recent publications [19–22] the amplitude dependence is shown to be an important feature for MS rubber even at small strains. Moreover, magnetic sensitivity is shown to be strongly amplitude dependent, why the inclusion of such effects in a model is essential to accurately reflect the physical phenomena. While beyond the scope of this work, a correct model will also provide valuable guidance when delving into the microscopical world trying to comprehend the underlying mechanisms ruling the macroscopical behaviour. The goal here is thus to create a phenomenological model correctly describing the different physical phenomena inherent to MS rubber in the audible frequency range, including viscoelasticity, amplitude dependence and also, the amplitude dependent magnetic sensitivity.

2. Model

The magneto-sensitive rubber is assumed homogeneous at the length scale considered, isotropic at no applied magnetic field and non-ageing while confined to isothermal conditions at room temperature—during the experiments the rubber temperature increase was within one degree. The study is furthermore confined to small strains excluding finite deformations, as the prime focus is on the small strain audio frequency applications at no static prestrain. The total stress response is assumed to be additively decomposable into three parts depending on time t,

$$\tau = \tau_e + \tau_{ve} + \tau_f, \tag{1}$$

where the elastic stress $\tau_e(t)$ is linearly related to the instantaneous strain $\gamma(t)$, the viscoelastic stress $\tau_{ve}(t)$ is linearly related to the history of the strain rate and the friction stress $\tau_f(t)$ is nonlinearly related to the strain.

It is often desirable to study these relationships in the frequency domain where expressions are largely reduced in size and calculations simplified, especially if linearity can be assumed. This can be readily done without any loss of information for the elastic and viscoelastic components of linear nature. The nonlinear frictional component on the other hand, will react to a single frequency sinusoidal strain by yielding one stress component of the same frequency as the input, and an infinite number of overtones of odd multiple order of that input frequency. These overtones, however, decay rapidly in amplitude and can therefore be dropped in analyses when studying linearized relationships between input and output; the linearized shear modulus being an example of this. Once that linearization has been performed, the following frequency domain relation can be established:

$$G = \frac{\tilde{\tau}(\omega)}{\tilde{\gamma}(\omega)}, \tag{2}$$

where the $\tilde{\cdot}$ symbol is henceforth employed for frequency domain quantities obtained by applying the temporal Fourier transform $\tilde{(\cdot)} = \int_{-\infty}^{\infty} (\cdot)\exp(-\mathrm{i}\omega t)\,\mathrm{d}t$; ω is the angular frequency in radians per second and G the linearized shear modulus in the frequency domain.

For the discussed relations accurate models exist which are employed in the modeling. Extending these models to the case of magneto-sensitive elastomers is the goal of this work. The primary challenge consists in determining the magneto-sensitivity of the respective parts and parameters.

2.1. Elastic part

The elastic dependence is simply described by

$$\tau_e = G_e\gamma, \tag{3}$$

where G_e is the elastic shear modulus.

2.2. Viscoelastic part

The viscoelastic dependence is suitably described by a relaxation convolution integral as

$$\tau_{\mathrm{ve}} = \int_{-\infty}^{t} G_{\mathrm{ve}}(t-s)\frac{\partial\gamma(s)}{\partial s}\,\mathrm{d}s, \tag{4}$$

where G_{ve} is a viscoelastic relaxation function obeying $\lim_{s\to\infty} G_{\mathrm{ve}}(s) = 0$ and $G_{\mathrm{ve}}(s) = 0$ for $s < 0$. In particular, the relaxation function is conveniently modeled as $G_{\mathrm{ve}} = bI_\alpha$ where the Abel operator kernel

$$I_\alpha(t) = \frac{h(t)}{t^\alpha \Gamma(1-\alpha)}, \tag{5}$$

$0<\alpha\leq 1$ and $b>0$ are material constants, h is a step function and Γ is the gamma function. This relation is possible to identify with a fractional derivative example

$$\tau_{ve}=\frac{b}{\Gamma(1-\alpha)}\frac{d}{dt}\int_{-\infty}^{t}\frac{\gamma(s)}{(t-s)^{\alpha}}\,ds, \tag{6}$$

with a minimum number of parameters required to successfully model wide-frequency band rubber properties [23]. This can numerically be evaluated accordingly

$$\tau_{ve}\approx b\frac{\Delta t^{-\alpha}}{\Gamma(-\alpha)}\sum_{m=0}^{n-1}\frac{\Gamma(m-\alpha)}{\Gamma(m+1)}\gamma_{n-m}, \tag{7}$$

where $t_n=n\Delta t, \gamma_n=\gamma(t_n)$ and Δt is a constant time step used in the estimation process and $\gamma(s)=0$ for $s<0$.

2.3. Frictional part

The amplitude dependence is expressed by means of a smooth frictional stress model expressed as [24]

$$\tau_f=\tau_{fs}+\frac{\gamma-\gamma_s}{\gamma_{1/2}\left[1-\mathrm{sign}(\dot\gamma)\frac{\tau_{fs}}{\tau_{fmax}}\right]+\mathrm{sign}(\dot\gamma)[\gamma-\gamma_s]}[\tau_{fmax}-\mathrm{sign}(\dot\gamma)\tau_{fs}], \tag{8}$$

where the maximum friction stress developed τ_{fmax} and $\gamma_{1/2}$ are model constants with $\mathrm{sign}(\dot\gamma)$ yielding the direction of the displacement. The parameters τ_{fs} and γ_s are updated each time there is a change in shear direction at $\dot\gamma_s=0$ as $\tau_{fs}\leftarrow\tau_f|_{\dot\gamma=0}$ and $\gamma_s\leftarrow\gamma|_{\dot\gamma=0}$.

2.4. Frequency dependent shear modulus

The relations in Sections 2.1–2.3 are time domain functions. However, for a sinusoidal strain excitation, results are more easily visualized in the frequency domain why those functions are Fourier transformed in order to arrive at the desired frequency dependent shear modulus (2). As previously mentioned, overtones will appear in the frictional stress part once it has been transformed; these will be dropped in order to obtain the necessary linearized relation between stress and strain, ultimately providing the complex frequency dependent shear modulus. It should be noted that although the shear modulus derives from a linearized relation, it is nonetheless nonlinear, exhibiting a strong amplitude dependence.

2.5. Parameter values and magnetic sensitivity

Upon application of a magnetic field the material becomes anisotropic as the shear modulus is dependent of the direction of the magnetic field. Three experimental observations [19–22] form the frames for the inclusion of magneto-sensitivity in the current model where the magnetic field is assumed perpendicular to the shear direction. Firstly, not only does the material display a strong amplitude dependence even for small strains—reflected in the choice of $\gamma_{1/2}$ and τ_{fmax}—but also the magnetic sensitivity displays a strong amplitude dependence. This suggests varying the frictional parameters for an accurate description of that phenomenon. Secondly, the shear modulus magnitude difference between the zero-field and saturated state at different frequencies appears in experiments to be relatively constant. This leads to the conclusion that in this model the viscoelastic dependence on magnetic induction can be neglected leaving b and α unchanged. Thirdly, the relatively small variation of the loss factor with magnetic field suggests that the loss increase that altering the frictional parameters gives rise to, be balanced by an increase in the elastic modulus G_e. Magnetic sensitivity should accordingly be introduced in connection with $\gamma_{1/2}, \tau_{fmax}$ and G_e.

Generally $B=B(H)$, where B is the magnetic flux density and H the magnetic field intensity. The relation is $B=\mu H$ where μ is the permeability of the medium. This can also be expressed as $B=\mu_0(H+M)$ where μ_0 is the permeability of free space and M the magnetization. Since B,H and M are perpendicular to the shear direction, M will subsequently appear as a scalar, only working uniaxially. Since physically, G must be an even function of M, this suggests the use of expressions of even powers of M; the simplest one being quadratic. Experiments have shown that G_e and τ_{fmax} increase with magnetic field, while $\gamma_{1/2}$ instead decreases.

The three magneto-sensitive parameters are expressed accordingly

$$G_e=\left[1+\left(\frac{M}{M_s}\right)^2\delta_1\right]G_{e0}, \tag{9}$$

$$\gamma_{1/2}=\frac{\gamma_{1/20}}{1+\left(\frac{M}{M_s}\right)^2\delta_2}, \tag{10}$$

and

$$\tau_{\mathrm{fmax}} = \left[1 + \left(\frac{M}{M_s}\right)^2 \delta_3\right] \tau_{\mathrm{fmax0}}, \tag{11}$$

where $\mu_0 M_s$ represents the saturation magnetization—the highest value $\mu_0 M$ can assume—and δ_1, δ_2 and δ_3 are real and positive material constants to be decided. The parameters $G_{e\,0}, \gamma_{1/20}$ and τ_{fmax0} represent, respectively, the zero state values. In all, the number of parameters in the model amount to nine, including, apart from the six above ones, also b, α and $\mu_0 M_s$.

3. Results—comparison with experimental results

The parameters $G_e, b, \alpha, \gamma_{1/2}$ and τ_{fmax} are in the initial phase ascribed values; at this stage where M equals zero, the model represents the behaviour of the material as yet unaltered by the application of a magnetic field. Optimizing parameters with respect to the experimentally obtained zero-field curves [22] in Figs. 1–8 results in the following values: G_{e0}=1.35 MN m^{-2}, b=0.12 MN m^{-2} s$^{\alpha}$, $\alpha = 0.36, \gamma_{1/20} = 0.00103$ and $\tau_{\mathrm{fmax0}} = 0.9$ kN m^{-2}. Next $\delta_1, \delta_2, \delta_3$ and $\mu_0 M_s$ are ascribed values fitting the model to the three topmost curves in Fig. 1 and the corresponding curves in Fig. 2, representing the smallest strain shear modulus for the three magnetically altered states. These parameters are, respectively, given the values of $\delta_1 = 0.80, \delta_2 = 2.50, \delta_3 = 0.55$ and $\mu_0 M_s = 0.6$ T. The modeled results are seen to correspond well with experimental ones. In Figs. 9 and 10 modeled hysteresis loops are compared with corresponding hysteresis measurements. Modeled results are plotted in full lines. The parameter values are the same as the ones used in the shear modulus analysis

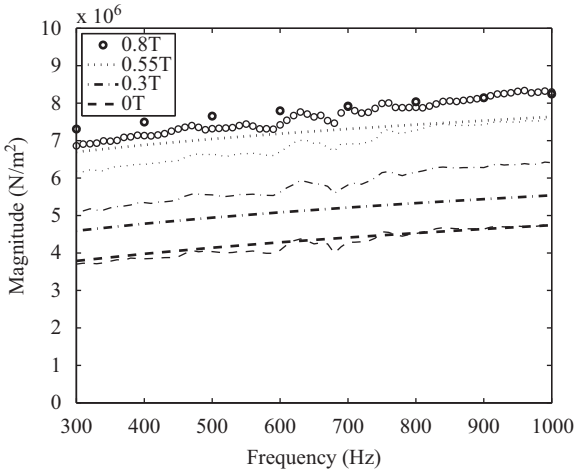

Fig. 1. Experimentally obtained shear modulus magnitude $|G|$ (thin lines) and corresponding modeled results (thick lines) versus frequency at induced magnetic field of 0, 0.3, 0.55 and 0.8 T for NR 33 percent Fe subjected to a shear strain of 0.000085.

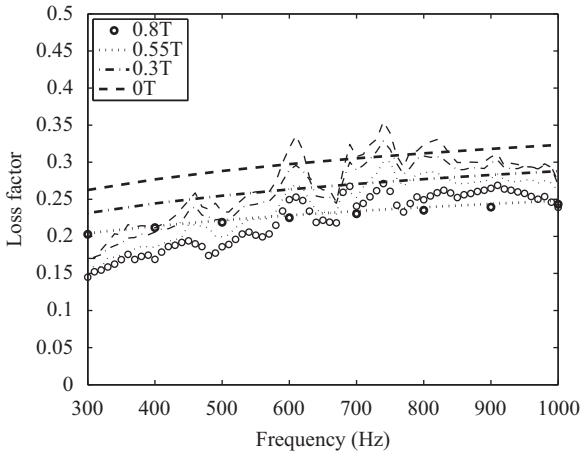

Fig. 2. Experimentally obtained shear modulus loss factor Im G/Re G (thin lines) and corresponding modeled results (thick lines) versus frequency at induced magnetic field of 0, 0.3, 0.55 and 0.8 T for NR 33 percent Fe subjected to a shear strain of 0.000085.

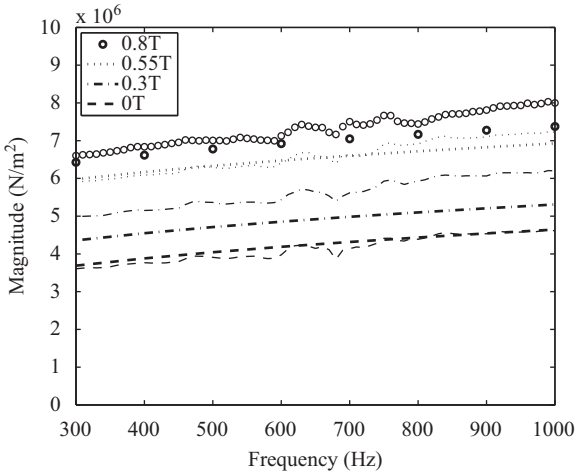

Fig. 3. Experimentally obtained shear modulus magnitude $|G|$ (thin lines) and corresponding modeled results (thick lines) versus frequency at induced magnetic field of 0, 0.3, 0.55 and 0.8 T for NR 33 percent Fe subjected to a shear strain of 0.00021.

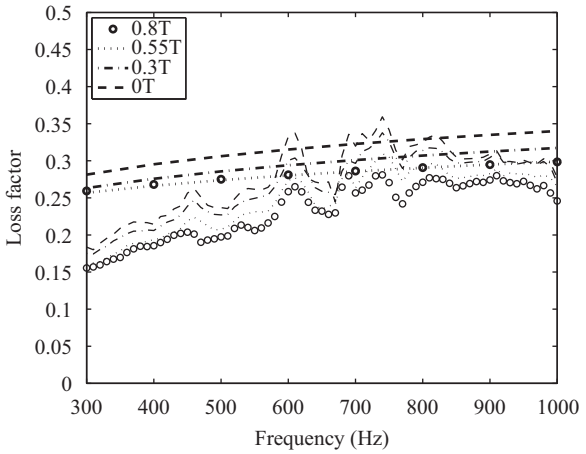

Fig. 4. Experimentally obtained shear modulus loss factor Im G/Re G (thin lines) and corresponding modeled results (thick lines) versus frequency at induced magnetic field of 0, 0.3, 0.55 and 0.8 T for NR 33 percent Fe subjected to a shear strain of 0.00021.

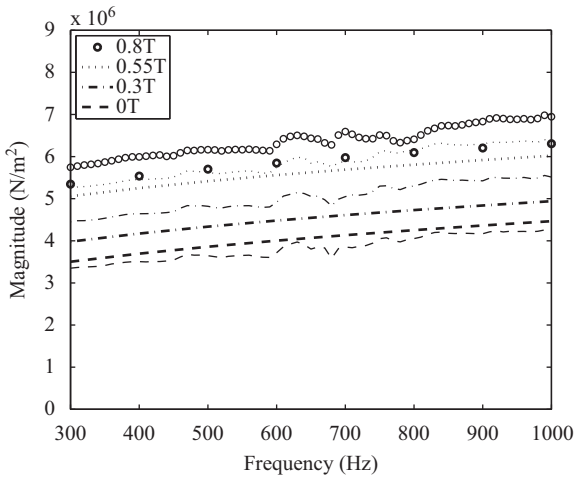

Fig. 5. Experimentally obtained shear modulus magnitude $|G|$ (thin lines) and corresponding modeled results (thick lines) versus frequency at induced magnetic field of 0, 0.3, 0.55 and 0.8 T for NR 33 percent Fe subjected to a shear strain of 0.00065.

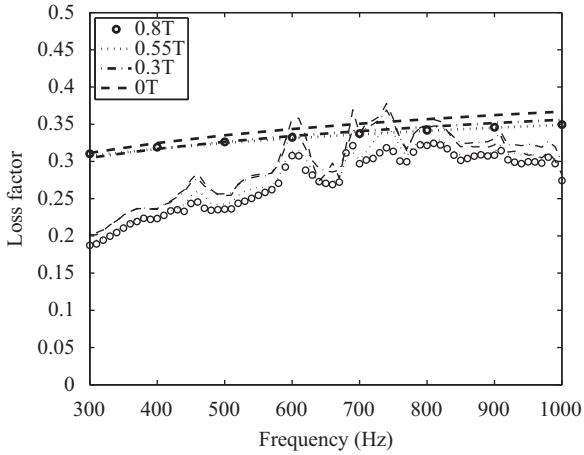

Fig. 6. Experimentally obtained shear modulus loss factor Im G/Re G (thin lines) and corresponding modeled results (thick lines) versus frequency at induced magnetic field of 0, 0.3, 0.55 and 0.8 T for NR 33 percent Fe subjected to a shear strain of 0.00065.

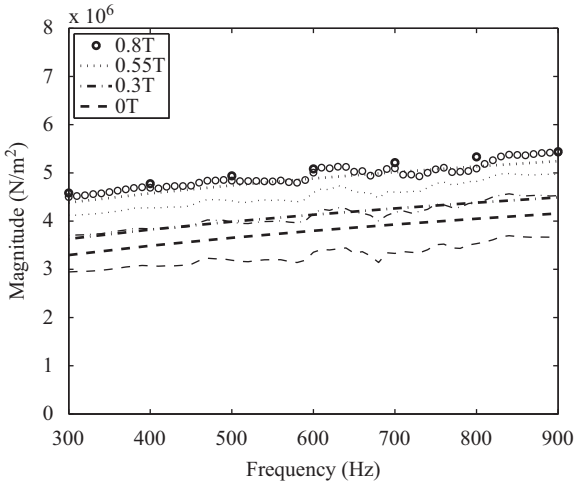

Fig. 7. Experimentally obtained shear modulus magnitude $|G|$ (thin lines) and corresponding modeled results (thick lines) versus frequency at induced magnetic field of 0, 0.3, 0.55 and 0.8 T for NR 33 percent Fe subjected to a shear strain of 0.0021.

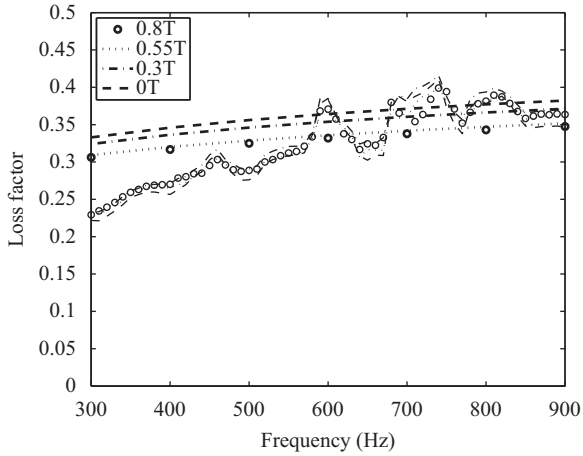

Fig. 8. Experimentally obtained shear modulus loss factor Im G/Re G (thin lines) and corresponding modeled results (thick lines) versus frequency at induced magnetic field of 0, 0.3, 0.55 and 0.8 T for NR 33 percent Fe subjected to a shear strain of 0.0021.

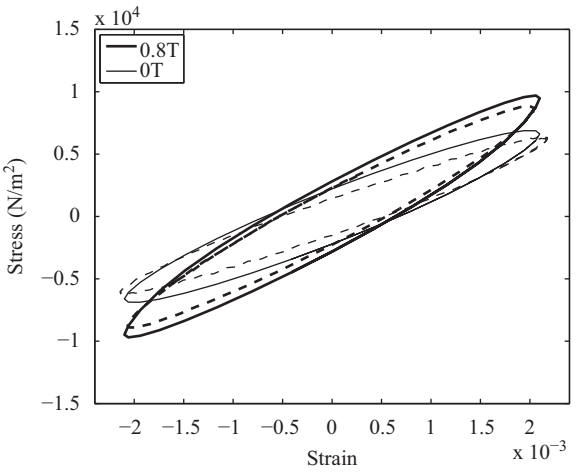

Fig. 9. Experimentally obtained time plot (thin lines) at the fixed frequency 300 Hz of stress versus strain at induced magnetic fields of 0 and 0.8 T and corresponding modeled results (thick lines) for NR 33 percent Fe subjected to a shear strain of 0.0021.

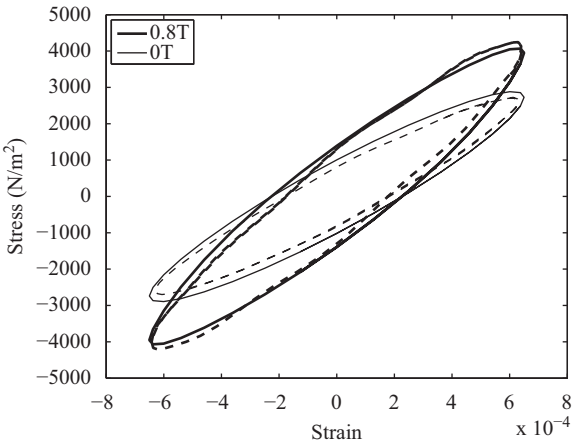

Fig. 10. Experimentally obtained time plot at the fixed frequency 1000 Hz of stress versus strain at induced magnetic fields of 0 and 0.8 T and corresponding modeled results (thick lines) for NR 33 percent Fe subjected to a shear strain of 0.00065.

yielding results corresponding well to experimental ones. While expected in the sense that the rubber samples subjected to the stepped sine and hysteresis measurements are the same—the difference naturally being that the measurements are not performed simultaneously—it does nevertheless lend further credibility to the model since in contrast to the shear modulus measurements and model, overtones are retained, which if not properly reflected in the model would not yield the characteristic shape at the turn points of each loop, but rather the viscoelastic shape of a perfect ellipse. The tendency towards that latter behaviour can be observed in Fig. 10 where the amplitude is smaller than in Fig. 9 and the frictional component due to its nature tends to a linear loss-free elastic one, since the strain is smaller. In the figures the modeled loss factor is somewhat higher at low frequencies than for the corresponding experimental loss factor. This is due to the fact that in the measurements the charge amplifier utilized introduces a displacement phase lag at low frequencies, causing a slight decrease in loss factor.

4. Conclusion

A model of magneto-sensitive rubber in the audible frequency range is presented. In contrast to the large majority of existing magneto-sensitive elastomer models, this one involves viscoelasticity. Moreover, it accounts for the nonlinear amplitude dependence usually neglected in static, quasi-static and dynamic models for small strains. Furthermore, the former feature has recently been found to be not only very strong in itself, even for small strains—strains are usually of small magnitude in the audible frequency range—but also very magneto-sensitive, strongly affecting the resultant behaviour. This prompts the presence of that phenomenon in the model, and indeed, a very good agreement with experimentally obtained results is observed.

Acknowledgement

The gratefully acknowledged financial support is provided from the Swedish Research Council (Contract no: 621-2002-5643).

References

[1] J. Rabinow, The magnetic fluid clutch, *American Institute of Electrical Engineers* 67 (1948) 1308–1315.
[2] W.M. Winslow, Induced fibration of suspensions, *Journal of Applied Physics* 20 (1949) 1137–1140.
[3] A. Occhiuzzi, M. Spizzuoco, G. Serino, Experimental analysis of magnetorheological dampers for structural control, *Smart Materials and Structures* 12 (2003) 703–711.
[4] J.D. Carlson, M.R. Jolly, MR fluid, foam and elastomer devices, *Mechatronics* 10 (2000) 555–569.
[5] M. Yalcintas, H. Dai, Vibration suppression capabilities of magnetorheological materials based adaptive structures, *Smart Materials and Structures* 13 (2004) 1–11.
[6] Y. Hu, Y.L. Wang, X.L. Gong, X.Q. Gong, Z.X. Zhang, W.Q. Jiang, P.Q. Zhang, Z.Y. Chen, New magnetorheological elastomers based on polyurethane/Si-rubber hybrid, *Polymer Testing* 24 (3) (2005) 324–329.
[7] S.A. Demchuk, V.A. Kuz'min, Viscoelastic properties of magnetorheological elastomers in the regime of dynamic deformation, *Journal of Intelligent Material Systems and Structures* 75 (2) (2002) 396–400.
[8] G.Y. Zhou, Q. Wang, Study on the adjustable rigidity of magnetorheological-elastomer-based sandwich beams, *Smart Materials and Structures* 15 (2006) 59–74.
[9] F.D. Goncalves, M. Ahmadian, J.D. Carlson, Investigating the magnetorheological effect at high flow velocities, *Smart Materials and Structures* 15 (2006) 75–85.
[10] C. Carmignani, P. Forte, E. Rustighi, Design of a novel magneto-rheological squeeze-film damper, *Smart Materials and Structures* 15 (2006) 164–170.
[11] P. Blom, L. Kari, Smart audio frequency energy flow control by magneto-sensitive rubber isolators, *Smart Materials and Structures* 17 (2008) Article number: 015043.
[12] L.C. Davis, Model of magnetorheological elastomers, *Journal of Applied Physics* 85 (1999) 3348–3351.
[13] I.A. Brigadnov, A. Dorfmann, Mathematical modeling of magneto-sensitive elastomers, *International Journal of Solids and Structures* 40 (2003) 4659–4674.
[14] A. Dorfmann, R.W. Ogden, Magnetoelastic modelling of elastomers, *European Journal of Mechanics A—Solids* 22 (2003) 497–507.
[15] A. Dorfmann, R.W. Ogden, Nonlinear magnetoelastic deformations, *Quarterly Journal of Mechanics and Applied Mathematics* 57 (4) (2004) 599–622.
[16] S.V. Kankanala, N. Tryantafyllidis, On finitely strained magnetorheological elastomers, *Journal of the Mechanics and Physics of Solids* 52 (2004) 2869–2908.
[17] Y. Shen, M.F. Golnaraghi, G.R. Heppler, Experimental research and modeling of magnetorheological elastomers, *Journal of Intelligent Material Systems and Structures* 15 (1) (2004) 27–35.
[18] W.P. Fletcher, A.N. Gent, Non-linearity in the dynamic properties of vulcanised rubber compounds, *Transactions of the Institution of the Rubber Industries* 29 (1953) 266–280.
[19] J.M. Ginder, S.M. Clark, W.F. Schlotter, M.E. Nichols, Magnetostrictive phenomena in magnetorheological elastomers, *International Journal of Modern Physics B* 16 (17–18) (2002) 2412–2418.
[20] C. Bellan, G. Bossis, Field dependence of viscoelastic properties of MR elastomers, *International Journal of Modern Physics B* 16 (17–18) (2002) 2447–2453.
[21] G. Bossis, E. Coquelle, P. Kuzhir, Adaptive magnetorheological materials, *Annales de Chimie Science de Matériaux* 29 (6) (2004) 43–54.
[22] P. Blom, L. Kari, Amplitude and frequency dependence of magneto-sensitive rubber in a wide frequency range, *Polymer Testing* 24 (2005) 656–662.
[23] R. L Bagley, P.J. Torvik, Fractional calculus—a different approach to the analysis of viscoelastically damped structures, *American Institute of Aeronautics and Astronautics Journal* 21 (1983) 741–748.
[24] M. Sjöberg, L. Kari, Nonlinear isolator dynamics at finite deformations: an effective hyperelastic, fractional derivative, generalized friction model, *Nonlinear Dynamics* 33 (3) (2003) 323–336.